Observational Study

Medicine®

OPEN

# Revealing the action mechanisms of dexamethasone on the birth weight of infant using RNA-sequencing data of trophoblast cells

Hongkai Shang, MD[a], Liping Sun, BM[a], Thorsten Braun, MD[b], Qi Si, BM[a], Jinyi Tong, MM[a,*]

**Abstract**

Dexamethasone (DEX) could induce low birth weight of infant, and low birth weight has close associations with glucocorticoid levels, insulin resistance, hypertension, and metabolic syndrome in adulthood. This study was designed to reveal the action mechanisms of DEX on the birth weight of infant.

Using quantitative real-time polymerase chain reaction (qRT-PCR), trophoblast cells of human placenta were identified and the optimum treatment time of DEX were determined. Trophoblast cells were treated by DEX (DEX group) or ethanol (control group) (each group had 3 samples), and then were performed with RNA-sequencing. Afterward, the differentially expressed genes (DEGs) were identified by R package, and their potential functions were successively enriched using DAVID database and Enrichr method. Followed by protein–protein interaction (PPI) network was constructed using Cytoscape software. Using Enrichr method and TargetScan software, the transcription factors (TFs) and micorRNAs (miRNAs) targeted the DEGs separately were predicted. Based on MsigDB database, gene set enrichment analysis (GSEA) was performed.

There were 391 DEGs screened from the DEX group. Upregulated *SRR* and potassium voltage-gated channel subfamily J member 4 (*KCNJ4*) and downregulated *GALNT1* separately were enriched in PDZ (an acronym of PSD-95, Dlg, and ZO-1) domain binding and Mucin type *O*-glycan biosynthesis. In the PPI network, CDK2 and CDK4 had higher degrees. TFs *ATF2* and *E2F4* and miRNA *miR-16* were predicted for the DEGs. Moreover, qRT-PCR analysis confirmed that *SRR* and *KCNJ4* were significantly upregulated.

These genes might affect the roles of DEX in the birth weight of infant, and might be promising therapeutic targets for reducing the side effects of DEX.

**Abbreviations:** $ATB^0$ = amino acid transport system $B^0$, BP = biological process, CC = cellular component, CDK2 = cyclin-dependent kinase 2, *CREB* = cAMP response-element binding protein, *CREM* = cAMP response-element modulator protein, DEGs = differentially expressed genes, DEX = Dexamethasone, DEX = Glucocorticoid dexamethasone, EGFR = epidermal growth factor receptor, Erk = extracellular signal-regulated kinase, ESC = embryonic stem cell, EVT = extravillus trophoblast, FPKM = fragments per kilobase million, GALNTL1 = *N*-acetylgalactosaminyltransferase-like 1, GALNTs = *N*-acetylgalactosaminyltransferases, *GAPDH* = glyceraldehyde-3-phosphate dehydrogenase, GO = gene ontology, *GLUT1* = glucose transporter 1, *GRα* = glucocorticoid receptor α, GSEA = gene set enrichment analysis, *IRS-1* = insulin receptor substrate-1, MAPK = mitogen-activated protein kinase, Mek = mitogen-activated protein kinase/ERK kinase, MF = molecular function, miRNAs = micorRNAs, mTOR = mechanistic target of rapamycin, *NMDAR* = NMDA receptor, PCA = principal component analysis, PCR = polymerase chain reaction, *PI3-K* = phosphatidylinositol 3-kinase, *PKB* = and protein kinase B, PPI = protein–protein interaction, qRT-PCR = quantitative real-time polymerase chain reaction, Rb = retinoblastoma protein, SEM = standard error of mean, *SRR* = serine racemase, STRING = Search Tool for the Retrieval of Interacting Genes, TFs = transcription factors, UCSC = University of California Santa Cruz.

**Keywords:** birth weight of infant, dexamethasone, protein–protein interaction network, regulatory network, trophoblast cells of human placenta

*Editor: Daryle Wane.*

*Competing interests: All authors declare that they have no competing interest to state.*

*This work was supported by National Natural Science Foundation of China (project number: 81601287), Natural Science Foundation of Zhejiang Province (project number: LQ15H040002), and Science and Technology Develop Project of Hangzhou (project number: 20140733Q06).*

*The authors have no conflicts of interest to disclose.*

*[a] Department of Obstetrics and Gynecology, Hangzhou First People's Hospital, Nanjing Medical University, Hangzhou, Zhejiang Province, China, [b] Department of Obstetrics and Gynecology, Charite Medical University, Berlin, Germany.*

*[*] Correspondence: Jinyi Tong, Department of Obstetrics and Gynecology, Hangzhou First People's Hospital, Nanjing Medical University, No. 261 Huansha Road, Hangzhou 310006, Zhejiang Province, China (e-mail: JinyiTong45@126.com).*



*Medicine (2018) 97:4(e9653)*

*Received: 15 May 2017 / Received in final form: 26 December 2017 / Accepted: 27 December 2017*

*http://dx.doi.org/10.1097/MD.0000000000009653*

## 1. Introduction

Premature delivery is an important factor that affects the morbidity and mortality of perinatals, with a incidence of 5% to 15%.[1] Premature infants have immature respiratory system and lack of pulmonary surfactant, thus their lives are seriously threatened.[2] For pregnant women in the 24th to 34th week and with the risk of giving birth prematurely, glucocorticoids are recommended for promoting fetal lung maturation.[3] However, glucocorticoids used in metaphase and terminal period can significantly reduce the birth weight and head circumference of infant.[4,5] On the other hand, the low birth weight of infant has close association with glucocorticoid levels, insulin resistance, hypertension, and metabolic syndrome in adulthood.[6] Therefore, revealing the action mechanisms of glucocorticoids on the birth weight of infant is critical for decreasing the side effects of glucocorticoids.

Glucose is an important nutrient in fetal growth and development, and glucose transporter 1 (*GLUT1*) and *GLUT3* separately play primary and secondary roles in glucose transport in placenta.[7] Several studies have found that glucocorticoids can reduce the expression of *GLUT* in placenta.[8–10] Glucocorticoid dexamethasone (DEX) decreases the expression level of glucocorticoid receptor α (*GRα*) through reducing the number of $GR\alpha^+$ binucleate cells, which varies with different fetal gender and gestational age.[11] DEX is reported to impair glucose transport capacity and induce insulin resistance through reducing insulin receptor substrate-1 (*IRS-1*), phosphatidylinositol 3-kinase (*PI3-K*), and protein kinase B (*PKB*).[12] However, the action mechanisms of DEX on the birth weight of infant have not yet been comprehensively reported.

In this study, the trophoblast cells of human placenta treated or untreated by DEX were used for RNA-sequencing. Subsequently, the differentially expressed genes (DEGs) were analyzed and predicted for their potential functions. Furthermore, protein–protein interaction (PPI) network analysis, regulatory network analysis, and gene set enrichment analysis (GSEA) were carried out for deeply exploring the target genes of DEX. In addition, quantitative real-time polymerase chain reaction (qRT-PCR) was applied for confirming the expression changes of key genes. This study might contribute to identify the therapeutic targets for reducing the side effects of DEX.

## 2. Methods

### 2.1. Identification of trophoblast cells and determination of the optimum treatment time of DEX

The trophoblast cells of human placenta used in this study were acquired from Cell bank of Chinese Academy of Sciences. Therefore, ethical approval and informed consent were not necessary. The cells were cultured in the Dulbecco's modified Eagle Medium/Ham's F-12 medium (DMEM/F12, GIBCO, Grand Island, NY) containing 10% fetal bovine serum (FBS, GIBCO, Grand Island, NY) and 1% penicillin/streptomycin double-antibody (GIBCO, Grand Island, NY) in a humidified incubator (at 37°C and 5% $CO_2$, Thermo Fisher Scientific Inc., MA). After the cells covered 80% to 90% of a culture dish, they were digested by pancreatin (GIBCO, Grand Island, NY), centrifuged, added with fresh medium, and then transferred to a new culture dish for passage. The trophoblast cells grew well were suspended in 2 mL DMEM/F12 medium (GIBCO, Grand Island, NY) in a 6-well plate and cultured in a humidified incubator (at 37°C and 5% $CO_2$, Thermo Fisher Scientific Inc., MA) for 24 hours. Followed by the cells in DEX group were treated by DEX (final concentration: 100 nM) for 24 hours, and the cells in control group were treated by the same volume of ethanol. Then, total RNA was extracted from the trophoblast cells using RNAiso Plus (Takara, Shiga, Japan) following the manufacturer's protocol, and were determinated using a spectrophotometer (NanoDrop Technologies, Wilmington, Delaware). Subsequently, RNA was reversely transcribed into the first-strand cDNA by a reverse transcription kit (TaKaRa, Tokyo, Japan) and stored for later use.

**Table 1**

**The primers used for polymerase chain reaction (PCR) experiments.**

| Primer name | Primer sequence (5′–3′) |
|---|---|
| GAPDH-F | TGACAACTTTGGTATCGTGGAAGG |
| GAPDH-R | AGGCAGGGATGATGTTCTGGAGAG |
| GLUT1-F | AACGCAACGAGGAGAAC |
| GLUT1-R | CGCAAACAGCGACACGAC |
| GLUT3-F | CCTTCCTCACTTCCATACAG |
| GLUT3-R | CTTAACCTCTCCAGCATCAA |
| HLA-E-F | CAGCATGAGGGGCTACCCG |
| HLA-E-R | GTGTGAGGAAGGGGGTCATG |
| KCNJ4-F | TGCTCTAATGTACTGCCATGGGAA |
| KCNJ4-R | CAGACCAGCCGAAGTCAGCAA |
| SRR-F | TGCTTAATGAGCCCAACACCT |
| SRR-R | TCCTTTTCTGCTTCGGCCTT |

*GAPDH*=glyceraldehyde-3-phosphate dehydrogenase, *GLUT1*=glucose transporter 1, HLA=histocompatibility leukocyte antigen, *KCNJ4*=potassium voltage-gated channel subfamily J member 4, PCR=polymerase chain reaction, *SRR*=serine racemase.

For polymerase chain reaction (PCR) experiments, the primers of histocompatibility leukocyte antigen-E (*HLA-E*), *GLUT1*, *GLUT3*, and glyceraldehyde-3-phosphate dehydrogenase (*GAPDH*) were designed using Primer Premier 6.0 software (Premier Software Inc., Cherry Hill, NJ) and then synthesized by Sangon Biotech Co., Ltd (Sangon Biotech Co., Ltd., Shanghai, China) (Table 1). PCR was used to measure the expression level of *HLA-E* in trophoblast cells, and the amplification products were detected using 1.5% agarose gel electrophoresis. Besides, the expression levels of *GLUT1* and *GLUT3* in trophoblast cells were evaluated using SYBR green kit (Applied Biosystems, CA). The 20 μL reaction system included 10 μL SYBR Green Mix Buffer (2×), 2 μL cDNA solution (100 ng/μL), 0.4 μL forward primer (10 μM), 0.4 μL reverse primer (10 μM), and 7.2 μL RNase Free $ddH_2O$. The amplifying program was as follows: 95°C for 10 minutes; and 95°C for 15 seconds and 60°C for 60 seconds for 40 cycles; followed by a melting program of 95°C for 15 seconds, 60°C for 1 minute and 95°C for 15 seconds. *GAPDH* was selected as the reference gene, and each samples had 3 repeats.

### 2.2. RNA extraction and RNA-seq library construction

After the trophoblast cells were treated by DEX or the same volume of ethanol for 24 hours (each group had 3 samples), total RNA was extracted using RNAiso Plus (Takara, Shiga, Japan) and were detected using a spectrophotometer (NanoDrop Technologies, Wilmington, DE). After RNA-seq library construction was performed using NEBNext Ultra RNA Library Prep Kit for Illumina (New England Biolabs Inc., Beverly, MA), sequencing data were collected using the Illumina Hiseq 4000 platform (PE150) (Illumina, San Diego, CA). Finally, the sequencing data (accession number: SRP105013) were uploaded into the Sequence Read Archive (SRA) database.

### 2.3. Data preprocessing and DEGs screening

Based on FastQC (http://www.bioinformatics.babraham.ac.uk/projects/fastqc/) method,[13] quality control was carried out for the raw data. Based on Tophat (http://tophat.cbcb.umd.edu/)[14] and Cufflinks (http://cufflinks.cbcb.umd.edu)[15] software, the clean reads were assembled into transcripts. The hg19 reference genome in the University of California Santa Cruz (UCSC, https://genome.ucsc.edu) database and the hg19 RefGenes (a total of 25575 genes) were used as reference genome and reference transcriptome, respectively. Cufflinks software[15] was used to assemble and identify novel transcripts for non-RefGenes. Subsequently, sample normalization and calculation of The Fragments Per Kilobase Million (FPKM) for the genes in the 2 groups were performed using Cufflinks software.[15] After the FPKM values were performed with log 2 transformation, the *t*-test method[16] in R package (https://www.r-project.org/) was used to identify the DEGs between DEX and control groups. The threshold of $P$-value $< .05$ was used for selecting DEGs. Moreover, the hclust method[17] in R package was used to performing hierarchical cluster analysis for the DEGs. In addition, principal component analysis (PCA) was conducted using R software.[18]

### 2.4. Functional and pathway enrichment analysis

Using DAVID database (http://www.david.niaid.nih.gov),[19] GO (gene ontology, including 3 items: molecular function (MF), biological process (BP), and cellular component (CC))[20] functional and KEGG (Kyoto Encyclopedia of Genes and Genomes)[21] pathway enrichment analyses for the DEGs were conducted. The significant terms were selected with the thresholds of gene count $\geq 2$ and $P$-value $< .05$. To obtain more information, Enrichr method[22] (http://amp.pharm.mssm.edu/Enrichr/) was also used for performing GO[20] functional, as well as BioCarta,[23] KEGG,[21] Reactome, NCI-Nature_2016,[24] and Humancyc_2016[25] pathway enrichment analyses, with $P$-value $< .05$ as the threshold.

### 2.5. PPI network analysis

Search Tool for the Retrieval of Interacting Genes (STRING) database, which integrates both known and predicted PPIs of multiple organisms, can be applied for predicting functional interactions of proteins.[26] Using STRING database (http://string-db.org/),[26] PPIs were predicted for the proteins corresponding to the DEGs. The threshold for PPI prediction was combined score $> 0.4$. Then, Cytoscape software (http://www.cytoscape.org)[27] was used to construct the PPI network. Proteins in the PPI network were defined as network nodes, and the number of interactions involved them was taken as their degrees. In the PPI network, the hub nodes[28] were defined as nodes with relative higher degrees.

### 2.6. Regulatory network analysis

Based on the ENCODE_and_ChEA_Consensus_TFs_from_ChIP-X, ENCODE_TF_ChIP-seq_2015 and ChEA_2016 databases in Enrichr method,[22] transcription factors (TFs) were predicted for the DEGs, with the cut-off criterion of $P$-value $< .05$. Besides, TargetScan software (http://www.targetscan.org/vert_71/)[29] was used to predict microRNAs (miRNAs) for the DEGs. The $P$-value $< .05$ was set as the threshold. Finally, both TF-target and miRNA-target regulatory networks were visualized by Cytoscape software.[27]

### 2.7. Mining of deep knowledge

Based on Molecular Signature Database (MsigDB, http://www.broadinstitute.org/gsea/msigdb/index.jsp),[30] DEX-induced changes of biological functions, signaling pathways, and targets of TFs and miRNAs were identified by GSEA analysis[31] through performing randomized permutation test for whole transcriptome for 1000 times. The threshold was set as adjusted $P$-value $< .05$.

### 2.8. Validation of the expression changes of key genes

Using qRT-PCR experiments, the expression levels of serine racemase (*SRR*) and potassium voltage-gated channel subfamily J member 4 (*KCNJ4*) were also detected. The primers designed for *SRR* and *KCNJ4* were listed in Table 1. The experiments were performed as described above.

### 2.9. Statistical analysis

The $2^{-\Delta\Delta Ct}$ method[32] was utilized for calculating the expression levels of genes. All data were displayed as mean ± standard error of mean (SEM). Data analysis was performed using Graphpad prism (Graphpad Software, San Diego, CA). The threshold for significant difference was set as $P < .05$.

## 3. Results

### 3.1. Identification of trophoblast cells and determination of the optimum treatment time of DEX

PCR detected the specific expression of *HLA-E*, indicating that the cells were trophoblast cells of human placenta. qRT-PCR showed that the expression of both *GLUT1* (Fig. 1A) and *GLUT3* (Fig. 1B) were downregulated by DEX, especially in trophoblast cells treated by DEX for 24 hours ($P < .05$). Therefore, the optimum treatment time of DEX was considered as 24 hours and used for the following experiments.

### 3.2. DEGs analysis

After preprocessing of the raw data, a total of 391 DEGs (174 upregulated and 217 downregulated) were identified in the DEX group in relative to the control group. The number of upregulated genes was less than that of downregulated genes. PCA analysis indicated that the samples could be distinguished obviously (Fig. 2).

### 3.3. Functional and pathway enrichment analysis

Based on DAVID database, the DEGs were conducted with functional and pathway enrichment analyses. Functional enrichment analysis showed that the upregulated genes were enriched in PDZ domain binding (GO_MF; $P$-value = 2.82E−02; which involved *SRR* and *KCNJ4*) and Golgi cis cisterna (GO_CC, $P$-value = 4.43E−02). However, no significant pathways were enriched for the upregulated genes. For the downregulated genes, the enriched terms mainly included O-glycan processing (GO_BP, $P$-value = 3.25E−03), cytoplasm (GO_CC, $P$-value = 5.54E−04), amino acid binding (GO_MF, $P$-value = 2.27E−02),

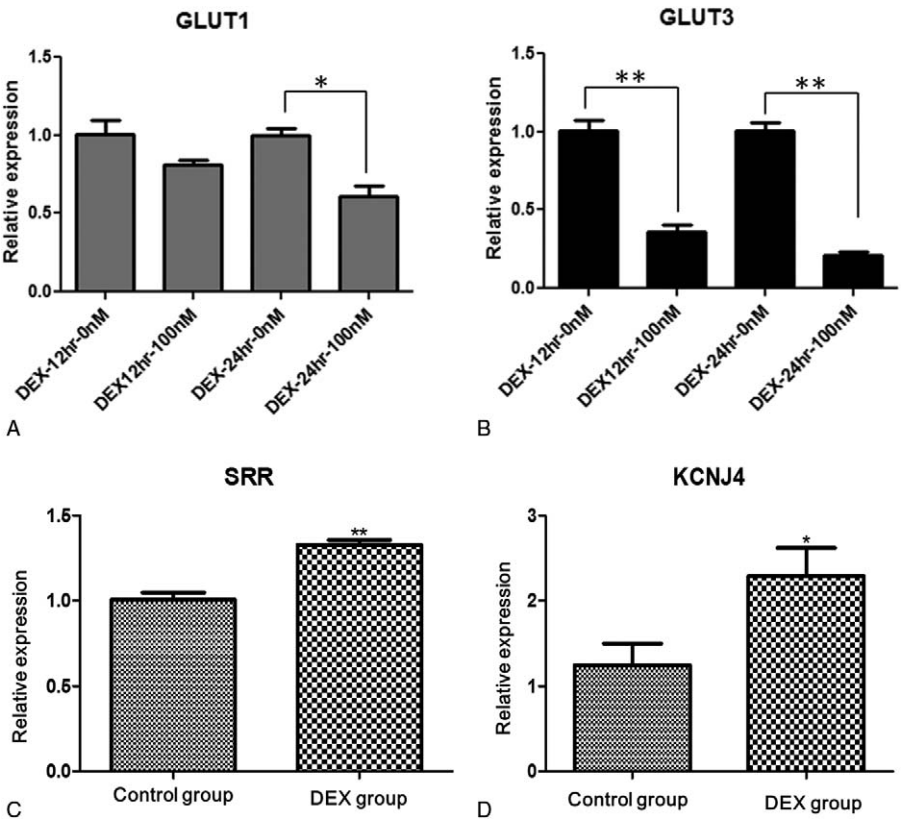


**Figure 1.** The relative expression of *GLUT1* (A) and *GLUT3* (B) in trophoblast cells treated by dexamethasone (DEX) for 12 hours or 24 hours, as well as the relative expression of *SRR* (C) and *KCNJ4* (D) in DEX and control groups. DEX = dexamethasone, *GLUT1* = glucose transporter 1.

and Mucin type *O*-glycan biosynthesis (pathway; *P*-value = 3.00E−03; which involved polypeptide *N*-acetylgalactosaminyl-transferase, *GALNT1*) (Table 2).

Meanwhile, enrichment analysis was also performed using Enrichr method. KEGG enrichment indicated that Glycan biosynthesis pathway was inhibited (Fig. 3A). Besides, NCI-Nature_2016 pathway enrichment showed that epidermal growth factor receptor (EGFR), mitogen-activated protein kinase (MAPK), mechanistic target of rapamycin (mTOR), and CD8 T signal transduction pathways were suppressed after DEX stimulation (Fig. 3B). Moreover, BioCarta pathway enrichment suggested that extracellular signal-regulated kinase (Erk), PI3K and mitogen-activated protein kinase/ERK kinase (Mek) signaling pathways were inhibited following DEX stimulation (Fig. 3C).

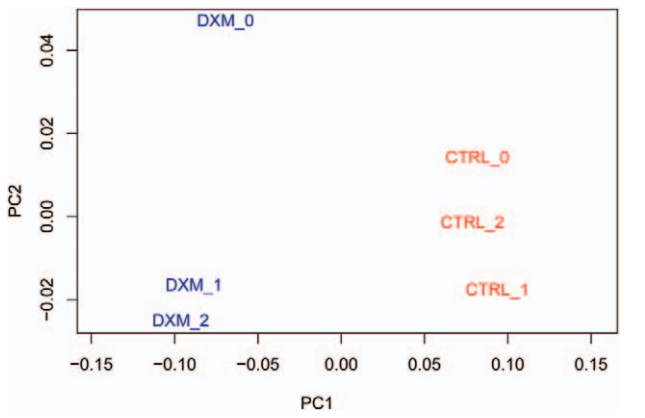


**Figure 2.** Principal component analysis (PCA) shows that dexamethasone and control samples can be separated obviously. PCA = principal component analysis.

### 3.4. Network analysis and mining of deep knowledge

For the DEGs, a PPI network involving 200 nodes and 287 interactions was constructed. Importantly, cyclin-dependent kinase 2 (CDK2) and CDK4 had higher degrees in the PPI network. After TFs (such as activating transcription factor 2, *ATF2*; and E2F transcription factor 4, *E2F4*) and miRNAs (such as *miR-16*) were predicted for the DEGs, the TF-target (Fig. 4) and miRNA-target (Fig. 5) regulatory networks separately were constructed.

Using GSEA analysis, DEX-induced changes of biological functions, signaling pathways, and targets of TFs and miRNAs were identified. Especially, the results showed that potassium channel activity was activated (Fig. 6) and ribosome pathway activity was suppressed (Fig. 7) by DEX.

### 3.5. qRT-PCR analysis to confirm the expression changes of key genes

qRT-PCR showed that the expression of both *SRR* (Fig. 1C) and *KCNJ4* (Fig. 1D) were significantly upregulated ($P < .05$), which was in accord with the results of DEGs analysis.

**Table 2**

**The GO terms (A) and pathways (B) enriched for the differentially expressed genes.**

**(A)**

| Category | Term | Count | *P*-value | Genes |
|---|---|---|---|---|
| Upregulated | | | | |
| GO_MF | GO:0030165–PDZ domain binding | 4 | 2.82E−02 | *ACVR2A, KCNJ4, CRIPT, SRR* |
| GO_CC | GO:0000137–Golgi cis cisterna | 2 | 4.43E−02 | *ATL1, GOLGA2* |
| Downregulated | | | | |
| GO_MF | GO:0016597–amino acid binding | 3 | 2.27E−02 | *SHMT2, AARS, KARS* |
| | GO:0005515–protein binding | 107 | 3.77E−02 | *OCLN, SNRPD3, LEMD3, RNF216, CXORF40A, AURKB, LZTFL1, ANKRD54, SLC2A4, APOH, RPRD1B, CRY1, RMND1, WWOX, EIF2B5, CHTOP, ZNF592, FAM21C, YY1, NCAPD2, MAPK1, TIMELESS, HHLA3, TWSG1, PPP2R3A, MPLKIP, HSD17B12, OAS1, KARS, EPM2AIP1, TMCC2, OAZ2, EIF3F, OTUD7B, CCDC22, SKA1, GNMT, DHX9, RAB8A, ZNF624, LAMTOR1, TBC1D10A, C22ORF39, ZMYM5, S100A11, NR4A3, RAB33B, REEP5, SEMA6A, DLX2, TULP3, SH3RF1, TLN1, VPS37B, MLH3, NAP1L4, MTFR2, GLB1, MAZ, TRIM9, RAB6A, STX5, ELP3, HIST1H1E, SULT2A1, AIFM1, DSN1, ZNF543, INCA1, ZNF143, CDK5, CDK2, DAPK1, SMU1, DOK3, LARP7, UBE2M, SLC41A3, MAPRE1, PRF1, PPP4R2, PCDHB14, PTPMT1, FEM1B, UBE2R2, SF3B2, HMMR, DDX19B, PER2, AGO3, MYCBP, SNRNP70, MTMR6, CCNB1IP1, PLP2, SHMT2, ATXN7L1, ISOC2, MIS12, CAPN1, PSMG1, WDR25, PYGL, SFPQ, CCDC117, CALM1, RCN2* |
| GO_CC | GO:0005737–cytoplasm | 73 | 5.54E−04 | *TLN1, MAEA, SNRPD3, VPS37B, NAP1L4, GLB1, ANKRD54, NANS, TRIM9, AIF1L, GDF9, RPRD1B, WWOX, EIF2B5, ELP3, FAM21C, SULT2A1, C2CD5, DSN1, SNUPN, YY1, AARS, INCA1, CDK5, CDK2, NCAPD2, DAPK1, SMU1, MAPK1, DOK3, AAAS, LARP7, UBE2M, ZNF383, MAPRE1, GPN2, PPP4R2, MPLKIP, HSD17B1, OAS1, FEM1B, KARS, PDSS2, EPM2AIP1, UBE2R2, OAZ2, CCDC125, KBTBD4, DDX19B, PER2, OTUD7B, AGO3, MYCBP, SNRNP70, GNMT, MTMR6, DHX9, SHMT2, ZMYM5, CHI3L1, SDSL, S100A11, ISOC2, PPA2, CAPN1, DRAM2, PSMG1, TULP3, PYGL, SFPQ, PARP3, FUK, CALM1* |
| | GO:0005634–nucleus | 74 | 9.86E−04 | *AKNA, HLF, ACOX1, GRPEL1, MAEA, RNF216, MLH3, AURKB, NAP1L4, TCEAL3, ANKRD54, MAZ, RPRD1B, CRY1, WWOX, ELMSAN1, EIF2B5, HIST1H1E, ZNF592, AIFM1, DSN1, RCOR2, SNUPN, YY1, ZNF543, ZNF189, INCA1, CDK5, CDK2, NCAPD2, SMU1, MAPK1, AAAS, TCFL5, TIMELESS, LARP7, ZNF383, RBM38, GLRX5, PPP4R2, MPLKIP, RABGAP1L, HOXB13, OAS1, PTPMT1, FEM1B, KARS, OAZ2, MEIS3, DDX19B, PER2, OTUD7B, TMEM192, MYCBP, SNRNP70, DHX9, SHMT2, RAB8A, ZNF624, FTO, KLF16, S100A11, NR4A3, ZNF221, ISOC2, MIS12, DLX2, PSMG1, TULP3, SFPQ, PARP3, NFIA, SDE2, CALM1* |
| | GO:0005829–cytosol | 49 | 2.67E−03 | *SH3RF1, TLN1, HSD17B1, SNRPD3, RNF216, OAS1, AURKB, RIOK2, LZTFL1, KARS, HMMR, OAZ2, THTPA, NANS, SLC2A4, EIF3F, AGO3, RAB6A, SKA1, GNMT, MTMR6, WWOX, DUS3L, EIF2B5, DHX9, STX5, CENPN, RAB8A, SULT2A1, FAM21C, EXOSC6, AIFM1, TBC1D10A, DSN1, SNUPN, AARS, CDK5, MIS12, CDK2, NCAPD2, CAPN1, MAPK1, PYGL, UBE2M, RBM38, MAPRE1, FUK, KIF26A, CALM1* |
| | GO:0005794–Golgi apparatus | 18 | 5.01E−03 | *SH3RF1, STX5, GALNT1, MPLKIP, LAMTOR1, RABGAP1L, GLB1, RAB33B, ST3GAL1, NRAS, MAPK1, PSMG1, DRAM2, LARP7, TMEM192, MAPRE1, RAB6A, WWOX* |
| | GO:0000818–nuclear MIS12/MIND complex | 2 | 1.95E−02 | *DSN1, MIS12* |
| | GO:0071011–precatalytic spliceosome | 3 | 2.48E−02 | *SNRPD3, SNRNP70, SF3B2* |
| | GO:0000139–Golgi membrane | 12 | 3.19E−02 | *ST3GAL1, NRAS, STX5, RAB8A, GALNT1, GCNT3, ST3GAL2, SLC35D2, CHST3, RAB6A, LPCAT2, RAB33B* |
| | GO:0005667–transcription factor complex | 6 | 4.20E−02 | *RCOR2, YY1, HOXB13, NR4A3, CDK2, ELMSAN1* |
| | GO:0005759–mitochondrial matrix | 8 | 4.31E−02 | *ACSM3, SHMT2, GLRX5, GRPEL1, PDE12, KARS, PPA2, PDSS2* |
| | GO:0000444–MIS12/MIND type complex | 2 | 4.82E−02 | *DSN1, MIS12* |
| GO_BP | GO:0016266–*O*-glycan processing | 5 | 3.25E−03 | *ST3GAL1, GALNT1, GCNT3, ST3GAL2, POFUT1* |
| | GO:0042754–negative regulation of circadian rhythm | 3 | 3.54E−03 | *SFPQ, PER2, CRY1* |
| | GO:0007062–sister chromatid cohesion | 6 | 4.05E−03 | *CENPN, DSN1, MAPRE1, SKA1, AURKB, MIS12* |
| | GO:0051301–cell division | 10 | 9.78E−03 | *MAEA, MPLKIP, TIMELESS, DSN1, MAPRE1, SKA1, CDK5, MIS12, CDK2, NCAPD2* |
| | GO:0042752–regulation of circadian rhythm | 4 | 1.36E−02 | *TIMELESS, SFPQ, PER2, CRY1* |
| | GO:0007067–mitotic nuclear division | 8 | 1.38E−02 | *CENPN, MPLKIP, TIMELESS, MAPRE1, SKA1, AURKB, MIS12, CDK2* |

(*continued*)

**Table 2**

**(continued).**

**(A)**

| Category | Term | Count | *P*-value | Genes |
|---|---|---|---|---|
| | GO:0000122–negative regulation of transcription from RNA polymerase II promoter | 15 | 1.55E−02 | *HIST1H1E, RCOR2, YY1, KLF16, ZNF189, NR4A3, AURKB, DLX2, TIMELESS, SFPQ, OTUD7B, PER2, CRY1, MEPCE, NFIA* |
| | GO:0048511–rhythmic process | 4 | 1.76E−02 | *DHX9, HLF, SFPQ, CDK5* |
| | GO:0021766–hippocampus development | 4 | 1.94E−02 | *DLX2, NR4A3, CDK5, EIF2B5* |
| | GO:0006464–cellular protein modification process | 5 | 2.24E−02 | *ST3GAL1, PPP4R2, ST3GAL2, UBE2M, GNMT* |
| | GO:0006913–nucleocytoplasmic transport | 3 | 2.65E−02 | *ANKRD54, AAAS, CDK5* |
| | GO:0008380–RNA splicing | 6 | 2.75E−02 | *PPP4R2, SFPQ, SNRPD3, RBM38, SNRNP70, SF3B2* |
| | GO:0060743–epithelial cell maturation involved in prostate gland development | 2 | 3.02E−02 | *HOXB13, FEM1B* |
| | GO:0010800–positive regulation of peptidyl-threonine phosphorylation | 3 | 3.06E−02 | *MAPK1, CHI3L1, CALM1* |
| | GO:0007059–chromosome segregation | 4 | 3.21E−02 | *CENPN, DSN1, SKA1, MIS12* |
| | GO:0018146–keratan sulfate biosynthetic process | 3 | 3.28E−02 | *ST3GAL1, ST3GAL2, SLC35D2* |
| | GO:0005975–carbohydrate metabolic process | 6 | 3.31E−02 | *GCNT3, SLC2A4, PYGL, CHI3L1, CHST3, GLB1* |
| | GO:0006397–mRNA processing | 6 | 3.63E−02 | *PPP4R2, PDE12, SFPQ, RBM38, SNRNP70, SF3B2* |
| | GO:0006493–protein *O*-linked glycosylation | 3 | 4.19E−02 | *GALNT1, GCNT3, POFUT1* |
| | GO:0010828–positive regulation of glucose transport | 2 | 4.99E−02 | *C2CD5, NR4A3* |

**(B)**

| Category | Term | Count | *P*-value | Genes |
|---|---|---|---|---|
| Downregulated | | | | |
| Pathway | hsa00512: Mucin type *O*-glycan biosynthesis | 4 | 3.00E−03 | *ST3GAL1, GALNT1, GCNT3, ST3GAL2* |
| | hsa00604: Glycosphingolipid biosynthesis–Ganglio series | 3 | 3.00E−03 | *ST3GAL1, ST3GAL2, GLB1* |
| | hsa01100: Metabolic pathways | 19 | 4.10E−02 | *ACOX1, GCNT3, GALNT1, SHMT2, HSD17B1, HSD17B12, SDSL, LPCAT2, PIGP, GLB1, ST3GAL1, ACSM3, THTPA, NANS, ST3GAL2, PYGL, FUK, MTMR6, ALG14* |
| | hsa04910:Insulin signaling pathway | 5 | 4.40E−02 | *MAPK1, NRAS, SLC2A4, PYGL, CALM1* |

BP = biological process, CC = cellular component, GO = gene ontology, MF = molecular function.


**Figure 3.** The results of KEGG (Kyoto Encyclopedia of Genes and Genomes) (A), NCI-Nature_2016 (B), and BioCarta (C) pathway enrichment analyses based on Enrichr method. KEGG= Kyoto Encyclopedia of Genes and Genomes.

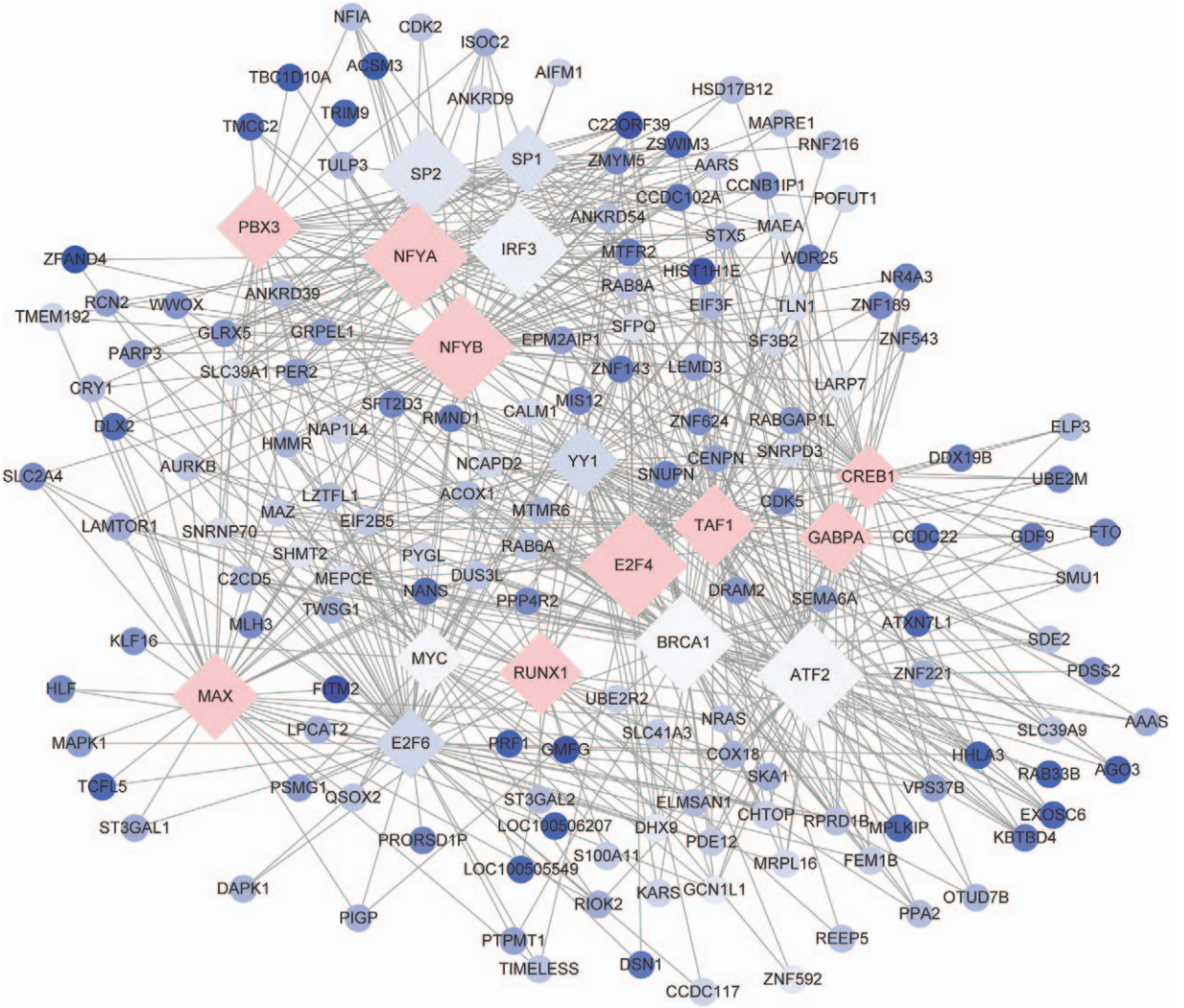


**Figure 4.** The transcription factor (TF)-target regulatory network. Red and blue represent upregulated genes and downregulated genes, respectively. Circles and diamonds separately represent genes and TFs. The shade of blue indicates fold change of downregulation. TF = transcription factor.

## 4. Discussion

After the trophoblast cells of human placenta were identified, the optimum treatment time of DEX was determined as 24 hours by qRT-PCR analysis. In this study, a total of 391 DEGs were identified in the DEX group compared with the control group, including 174 upregulated and 217 downregulated genes. Both DAVID database and Enrichr method were used for performing enrichment analysis. The PPI network for the DEGs was consisted of 200 nodes and 287 interactions. In addition, GSEA analysis showed that potassium channel activity was activated and ribosome pathway activity was suppressed by DEX. qRT-PCR analysis confirmed that *SRR* and *KCNJ4* were significantly upregulated in DEX group.

Functional enrichment analysis showed that upregulated *SRR* and *KCNJ4* were enriched in PDZ domain binding. *KCNJ2* gene is reported to have expression in human placenta and in all development and differentiation stages of cytotrophoblast cells.[33] Lockridge et al[34] demonstrated that *SRR* in peripheral tissues may be critical for glucose homeostasis, and D-serine in β-cells may act as an endogenous islet NMDA receptor (*NMDAR*) co-agonist. *SRR* mRNA is detected in placenta, and D-serine transported by amino acid transport system $B^0$ ($ATB^0$) has a higher circulating concentration in the fetus compared with the mother.[35] Meanwhile, pathway enrichment analysis showed that downregulated *GALNT1* was enriched in Mucin type O-glycan biosynthesis. The family of polypeptide *N*-acetylgalactosaminyltransferases (GALNTs) consists of 20 members, including GALNT1 to 14 and polypeptide *N*-acetylgalactosaminyltransferase-like 1 (GALNTL1) to L6.[36,37] Both *GALNT1* and *GALNT2* are overexpressed in first trimester extravillus trophoblast (EVT) and HTR8/SVneo cells, and the initiating enzyme of O-glycosylation *GALNT2* is important for mediating EVT invasion.[38] These declared that DEX might affect glucose transport in placenta through regulating *GALNT1* enriched in Mucin type O-glycan biosynthesis and *SRR* and *KCNJ4* enriched in PDZ domain binding.

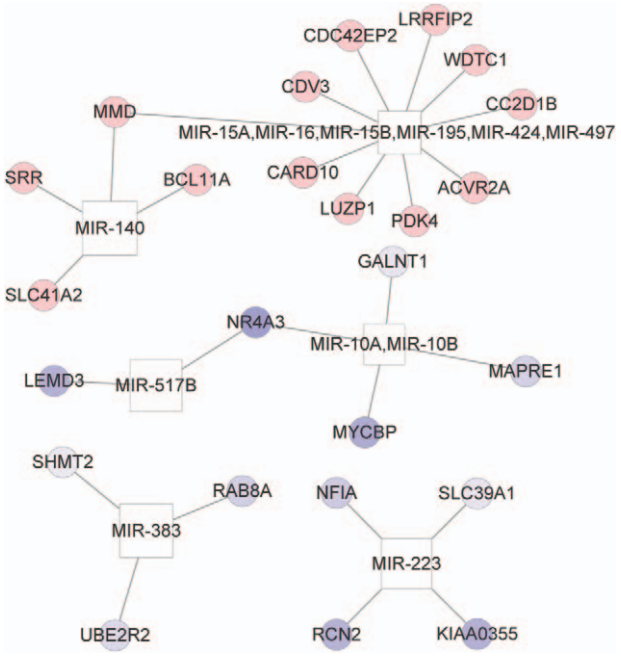


**Figure 5.** The microRNA (miRNA)-target regulatory network. Red and blue represent upregulated genes and downregulated genes, respectively. Circles and squares separately represent genes and miRNAs. The size of square indicates −log *P*-value of target genes.

Our results indicate that CDK2 and CDK4 were hub nodes in the PPI network. The simultaneous cytoplasmic mislocalization of *CDK2* and *p27* functions in regulating cell proliferation, invasion, and migration of human trophoblast cells.[39] *CDK2* expression patterns indicate the decreased cyclin-dependent kinase activity along with placental maturation, and the interactions of *CDK2*, cyclin E, *E2F1*, and $p27^{kip1}$ may mediate aberrant trophoblastic proliferations.[40] The knockouts of *CDK2* and *CDK4* can lead to embryonic lethality through inducing heart defects, and result in retinoblastoma protein (Rb) phosphorylation via regulating E2F-inducible genes.[41] The high activity of *CDK2* contributes to quickening G1 phase progression and establishing embryonic stem cell (ESC)-specific cell-cycle structure in mouse ESCs.[42] Therefore, *CDK2* and *CDK4* might also be implicated in the roles of DEX in trophoblast cells.

Moreover, TFs *ATF2* and *E2F4* and miRNA *miR-16* were predicted for the DEGs. Expression pattern changes of *ATF2*, cAMP response-element modulator protein (*CREM*), and cAMP response-element binding protein (*CREB*) have correlations with myometrial quiescence in the process of fetal maturation and uterine activation at term.[43–45] *E2F4* cooperates with *pRB* in placental development, and is essential for the development of multiple embryonic tissues.[46,47] Zhang et al[48] deem that *E2F4* interacted with *pRB* mediates cell cycle exit and plays a cell-intrinsic role during fetal erythropoiesis. *miR-16* and *miR-21* expression levels are obviously decreased in low birth weight infants and is correlated with fetal growth.[49] These suggested that *ATF2*, *E2F4*, and *miR-16* might also be targets of DEX during fetal maturation.

In conclusion, a total of 391 DEGs were identified in the DEX group. Besides, DEX might affect the birth weight of infant through mediating *GALNT1*, *SRR*, *KCNJ4*, *CDK2*, *CDK4*, *ATF2*, *E2F4*, and *miR-16*. However, our results were obtained from bioinformatics analysis and in vitro experiments of trophoblast cells. Therefore, more in-depth experiments should be conducted to further confirm these findings.

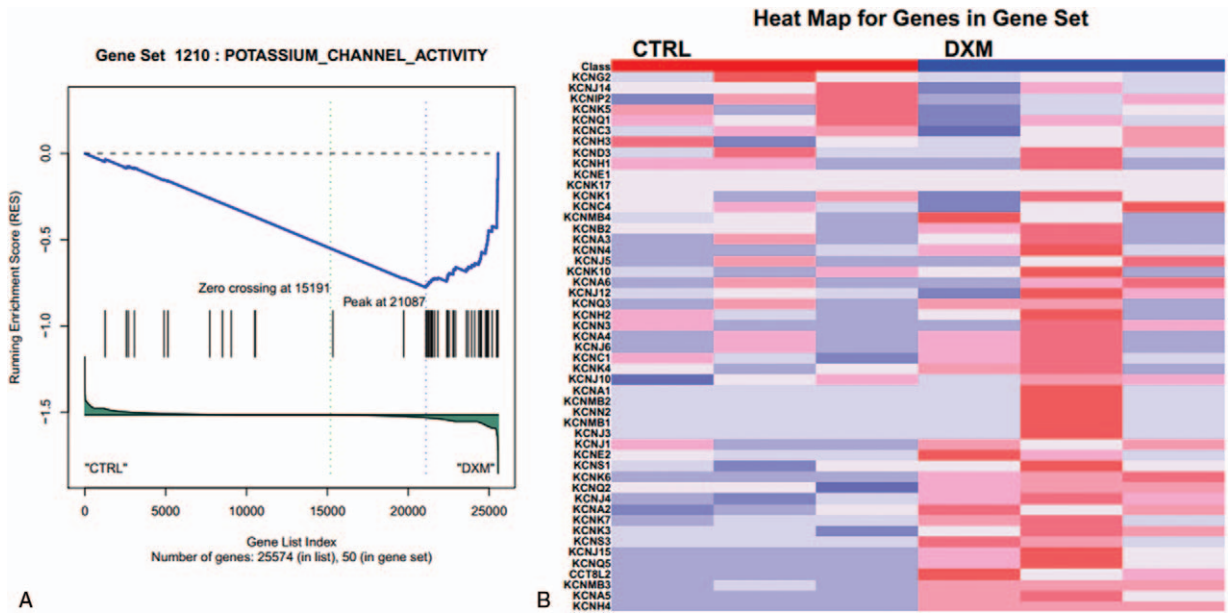


**Figure 6.** The gene set enrichment analysis (GSEA) result of POTASSIUM_ION_TRANSPORT (A) and the heatmap for the genes enriched in POTASSIUM_ION_TRANSPORT (B). GSEA = gene set enrichment analysis.

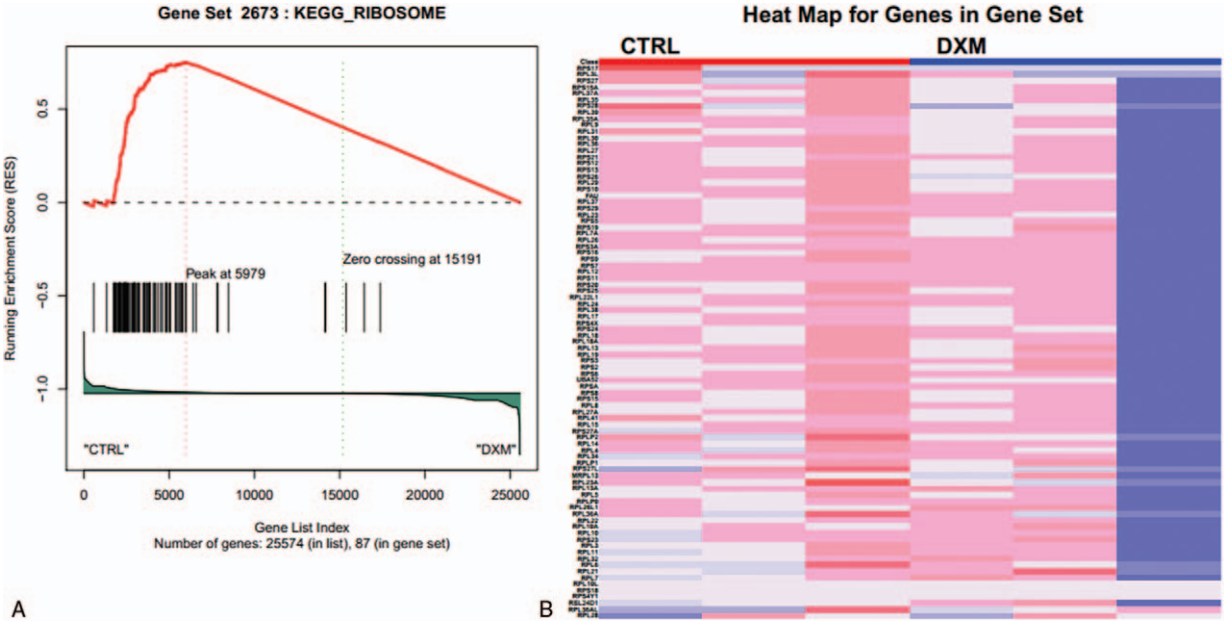


**Figure 7.** The gene set enrichment analysis (GSEA) result of KEGG_RIBOSOME (A) and the heatmap for the genes enriched in KEGG_RIBOSOME (B). GSEA = gene set enrichment analysis.

## References


[1] Lancet T. Preterm birth: crisis and opportunity. Lancet 2006;368: 339.

[2] Colin AA, McEvoy C, Castile RG. Respiratory morbidity and lung function in preterm infants of 32 to 36 weeks' gestational age. Pediatrics 2010;126:115.

[3] Mckinlay CJ, Crowther CA, Middleton P, et al. Repeat antenatal glucocorticoids for women at risk of preterm birth: a Cochrane Systematic Review. Am J Obstet Gynecol 2013;33:11–2.

[4] Harris A, Seckl J. Glucocorticoids, prenatal stress and the programming of disease. Horm Behav 2011;59:279–89.

[5] Barouki R, Gluckman PD, Grandjean P, et al. Developmental origins of non-communicable disease: Implications for research and public health. Environ Health 2012;11:42.

[6] Braun T, Challis JR, Newnham JP, et al. Early-life glucocorticoid exposure: the hypothalamic-pituitary-adrenal axis, placental function, and long-term disease risk. Endocrine Rev 2013;34:885.

[7] Novakovic B, Gordon L, Robinson WP, et al. Glucose as a fetal nutrient: dynamic regulation of several glucose transporter genes by DNA methylation in the human placenta across gestation. J Nutr Biochem 2013;24:282–8.

[8] Wyrwoll CS, Seckl JR, Holmes MC. Altered placental function of 11beta-hydroxysteroid dehydrogenase 2 knockout mice. Endocrinology 2009;150:1287–93.

[9] Brown K, Heller DS, Zamudio S, et al. Glucose transporter 3 (GLUT3) protein expression in human placenta across gestation. Placenta 2011; 32:1041–9.

[10] Khan H, Kusakabe KT, Wakitani S, et al. Quantitative expression and immunohistochemical detection of glucose transporters, GLUT1 and GLUT3 in the rabbit placenta during successful pregnancy. J Vet Med Sci 2011;73:1177–83.

[11] Shang H, Meng W, Sloboda DM, et al. Effects of maternal dexamethasone treatment early in pregnancy on glucocorticoid receptors in the ovine placenta. Reprod Sci 2015;22:534.

[12] Burén J, Liu HX, Jensen J, et al. Dexamethasone impairs insulin signalling and glucose transport by depletion of insulin receptor substrate-1, phosphatidylinositol 3-kinase and protein kinase B in primary cultured rat adipocytes. Eur J Endocrinol 2002; 146:419–29.

[13] Takeda H, Uesugi K, Mihara T, et al. A fast QC method for testing contact hole roughness by defect review SEM image analysis. IEEE T Semiconduct M 2008;21:567–72.

[14] Kim D, Pertea G, Trapnell C, et al. TopHat2: accurate alignment of transcriptomes in the presence of insertions, deletions and gene fusions. Genome Biol 2013;14:R36.

[15] Trapnell C, Williams BA, Pertea G, et al. Transcript assembly and quantification by RNA-seq reveals unannotated transcripts and isoform switching during cell differentiation. Nat Biotechnol 2010;28:511–5.

[16] Ruxton GD. The unequal variance t-test is an underused alternative to Student's t-test and the Mann–Whitney U test. Behav Ecol 2006; 17:688–90.

[17] Mahdavi M, Chehreghani MH, Abolhassani H, et al. Novel meta-heuristic algorithms for clustering web documents. Appl Math Comput 2008;201:441–51.

[18] German DM, Adams B, Hassan AE. The Evolution of the R Software Ecosystem. Proceedings of the 2013 17th European Conference on Software Maintenance and Reengineering 2013;88:243–52.

[19] Dennis G, Sherman BT, Hosack DA, et al. DAVID: database for annotation, visualization, and integrated discovery. Genome Biol 2003;4:3.

[20] Consortium TGO. Gene Ontology Consortium: going forward. Nucleic Acids Res 2015;43:1049–56.

[21] Kanehisa M, Sato Y, Kawashima M, et al. KEGG as a reference resource for gene and protein annotation. Nucleic Acids Res 2015;44:D457–62.

[22] Kuleshov MV, Jones MR, Rouillard AD, et al. Enrichr: a comprehensive gene set enrichment analysis web server 2016 update. Nucleic Acids Res 2016;44:W90–7.

[23] Chen YA, Hwang PI. Cross path-mapping pathways in KEGG or Biocarta with functional genomics data. J Genet Mol Biol 2006;17: 151–5.

[24] Schaefer CF, Anthony K, Krupa S, et al. PID: the pathway interaction database. Nucleic Acids Res 2009;37: D674–9.

[25] Trupp M, Altman T, Fulcher CA, et al. Beyond the genome (BTG) is a (PGDB) pathway genome database: HumanCyc. Genome Biol 2010; 11:1–11.

[26] Franceschini A, Szklarczyk D, Frankild S, et al. STRING v9. 1: protein–protein interaction networks, with increased coverage and integration. Nucleic Acids Res 2013;41:D808–15.

[27] Saito R, Smoot ME, Ono K, et al. A travel guide to Cytoscape plugins. Nat Methods 2012;9:1069–76.

[28] Liu X, Wang Y, Zhao D, et al. Patching by automatically tending to hub nodes based on social trust. Comput Stand Interfaces 2016;44:94–101.

[29] Lewis BP, Burge CB, Bartel DP. Conserved seed pairing, often flanked by adenosines, indicates that thousands of human genes are microRNA targets. Cell 2005;120:15.

[30] Liberzon A, Subramanian A, Pinchback R, et al. Molecular signatures database (MSigDB) 3.0. Bioinformatics 2011;27:1739.
[31] Subramanian A, Tamayo P, Mootha VK, et al. Gene set enrichment analysis: a knowledge-based approach for interpreting genome-wide expression profiles. Pro Natl Acad Sci USA 2005;102:15545–50.
[32] Arocho A, Chen B, Ladanyi M, et al. Validation of the 2−ΔΔCt calculation as an alternate method of data analysis for quantitative PCR of BCR-ABL P210 transcripts. Diagn Mol Pathol 2006;15:56–61.
[33] Riquelme G, Gregorio ND, Vallejos C, et al. Differential expression of potassium channels in placentas from normal and pathological pregnancies: targeting of the K ir 2.1 channel to lipid rafts. J Membr Biol 2012;245:141–50.
[34] Lockridge AD, Baumann DC, Akhaphong B, et al. Serine racemase is expressed in islets and contributes to the regulation of glucose homeostasis. Islets 2016;8:195–206.
[35] Chen Z, Huang W, Srinivas SR, et al. Serine racemase and D-serine transport in human placenta and evidence for a transplacental gradient for D-serine in humans. Reprod Sci 2004;11:294.
[36] Tarp MA, Clausen H. Mucin-type *O*-glycosylation and its potential use in drug and vaccine development. Biochim Biophys Acta 2008;1780: 546–63.
[37] Hagen KGT, Fritz TA, Tabak LA. All in the family: the UDP-GalNAc: polypeptide *N*-acetylgalactosaminyltransferases. Glycobiology 2003;13:1R.
[38] Liao WC, Chen CH, Liu CH, et al. Expression of GALNT2 in human extravillous trophoblasts and its suppressive role in trophoblast invasion. Placenta 2012;33:1005–11.
[39] Nadeem L, Brkic J, Chen YF, et al. Cytoplasmic mislocalization of p27 and CDK2 mediates the anti-migratory and anti-proliferative effects of nodal in human trophoblast cells. J Cell Sci 2013;126:445–53.
[40] Olvera M, Harris S, Amezcua CA, et al. Immunohistochemical expression of cell cycle proteins E2F-1, Cdk-2, Cyclin E, p27(kip1), and Ki-67 in normal placenta and gestational trophoblastic disease. Mod Pathol 2001;14:1036–42.
[41] Berthet C, Klarmann KD, Hilton MB, et al. Combined loss of Cdk2 and Cdk4 results in embryonic lethality and Rb hypophosphorylation. Dev Cell 2006;10:563.
[42] Koledova Z, Kafkova LR, Calabkova L, et al. Cdk2 inhibition prolongs G1 phase progression in mouse embryonic stem cells. Stem Cells Dev 2010;19:181–94.
[43] Bailey J, Sparey C, Phillips RJ, et al. Expression of the cyclic AMP-dependent transcription factors, CREB, CREM and ATF2, in the human myometrium during pregnancy and labour. Mol Hum Reprod 2000; 6:648.
[44] Breitwieser W, Lyons S, Flenniken AM, et al. Feedback regulation of p38 activity via ATF2 is essential for survival of embryonic liver cells. Genes Dev 2007;21:2069–82.
[45] Ackermann J, Ashton G, Lyons S, et al. Loss of ATF2 function leads to cranial motoneuron degeneration during embryonic mouse development. PLoS One 2011;6:e19090.
[46] Lee EY, Yuan TL, Danielian PS, et al. E2F4 cooperates with pRB in the development of extra-embryonic tissues. Dev Biol 2009;332:104–15.
[47] Berman SD. The Roles of Rb, p107, and E2f4 in Bone Formation and Embryonic Development. 2007;Massachusetts Institute of Technology,
[48] Zhang J, Lee EY, Liu Y, et al. pRB and E2F4 play distinct cell-intrinsic roles in fetal erythropoiesis. Cell Cycle 2010;9:371–6.
[49] Maccani MA, Padbury JF, Marsit CJ. miR-16 and miR-21 expression in the placenta is associated with fetal growth. PLoS One 2011;6:e21210.